ICPA 17th INTERNATIONAL CONFERENCE ON PRECISION AGRICULTURE
ConBAP CONGRESSO BRASILEIRO DE AGRICULTURA DE PRECISÃO E DIGITAL 2026
13-16 July 2026 | Porto Alegre, Brazil
ISPA AsBraAP

Sugarcane row gaps enable the identification of critical rows for targeted interventions

E.R.O. Silva[1], J.P. Molin[2], R. Canal Filho[2], M.R. Cherubin[3]

[1]Center for Carbon Research in Tropical Agriculture, "Luiz de Queiroz" College of Agriculture, University of São Paulo, SP, Brazil

[2]Laboratory of Precision Agriculture, "Luiz de Queiroz" College of Agriculture, University of São Paulo, SP, Brazil

[3]Department of Soil Science, "Luiz de Queiroz" College of Agriculture, University of São Paulo, SP, Brazil; Center for Carbon Research in Tropical Agriculture, University of São Paulo, SP, Brazil

A paper from the Proceedings of the
17th International Conference on Precision Agriculture and 11th Brazilian Congress on Precision and Digital Agriculture
13-15 July 2026
Porto Alegre, Brazil

Abstract

*Distinct patterns of sugarcane row gaps and associated plant population reduction drive the spatiotemporal variability of yield, creating a bottleneck for row prioritization in management decisions. This study tested the hypothesis that specific sugarcane rows within a field concentrate most of the linear gap lengths (LLG) and their associated economic and productive losses, consistent with the Pareto Principle. The objective was to identify rows that are critical in terms of LLG occurrence, making them priorities for site-specific interventions. Four case studies were conducted in sugarcane fields in the South-Central region of Brazil across distinct contexts, including one temporal assessment over two consecutive harvests. Subsequently, ten additional datasets were spatially investigated to strengthen the results. Yield data were obtained using sugarcane harvesters equipped with yield monitors and UAV-derived RGB mosaics were processed through automated row reconstruction and gap detection algorithms based on K-means segmentation guided by the L*a*b color space, producing row and gap maps. Production not obtained due to gap (P_g) was estimated at the row level, and two cost indicators were calculated: gap economic cost (GEC; expenses related to cultural practices, inputs, and land leasing) and gap opportunity cost (GOC; revenue associated with local yield). In each field, rows were ranked according to the sum of LLG, ranging from rows without gaps (less critical) to those with the highest LLG (more critical). Based on the Pareto Principle, the spatial distribution pattern of sugarcane row gaps was analyzed by the proportion of critical rows relative to total rows in each field. To quantify inequality in LLG distribution, the Gini coefficient (G) and the corresponding Lorenz curves were calculated. It was observed that 70% of the LLG was accumulated by 30-*

40% of the rows in fields at early production stages (1st to 3rd harvests), corroborating adherence to the Pareto Principle. Across the four case studies, the observed concentration of LLG was also reflected in P_g, GEC, and GOC, with 70% of these impacts concentrated in 30-40% of the rows. In fields at more advanced production stages, the same fraction of LLG required approximately 52-58% of the rows, indicating degradation of the Pareto-type pattern as the crop cycle progressed, which was supported by the temporal study (increase in the fraction of critical rows from the 3rd to the 4th harvest). Lorenz curves confirmed this behavior, positioned farther from the line of equality in fields with high Gini values (frequently G > 0.40, indicating well-defined critical rows in early harvests) and approaching this line in more advanced ratoon cycles (G = 0.18 to 0.39 in scenarios from the 4th harvest onward, indicating that sugarcane row gaps are more diffusely distributed within the field). By demonstrating the spatial concentration of row gaps and their economic impacts, the proposed approach supports strategic field management. Identifying critical rows enables economically prioritized interventions, particularly localized replanting in early cycles and renovation planning in advanced ratoon stages. This contributes to improved production efficiency and better resource allocation.

Keywords.

Economic losses, Image processing, Pareto Principle, UAV, Yield map

1. **Introduction**

Sugarcane (*Saccharum* spp.) plays a strategic role in global sugar, ethanol, and bioenergy production and is of high socioeconomic importance in tropical and subtropical regions. The global harvested area of sugarcane remains above 25 million hectares, while in Brazil, the area allocated for harvest is estimated at approximately 9.1 million hectares in the 2026/27 growing season, reinforcing the central role of this production chain in the agricultural and energy sectors (CONAB, 2026; FAOSTAT, 2026). In this context, the sugar-energy sector assumes increasing responsibilities in addressing sustainability challenges, particularly in improving production efficiency, promoting the rational use of inputs, and mitigating the effects of climate change on crop yield and raw material quality (Guhan et al., 2024; Raza et al., 2024).

Sugarcane field longevity is one of the cornerstones of crop management, as sugarcane is a perennial grass cultivated in semi-perennial cycles that typically last five to six years in tropical regions (Farhate et al., 2022). However, this longevity is continuously compromised by the occurrence of row gaps, defined as spaces where plants should be present but failed to establish or were lost throughout successive production cycles. These gaps result from factors such as harvesting damage, intensive machinery traffic, weed and pest infestations, disease occurrence, and other environmental and management-related constraints (Mahadea-Nemdharry et al., 2025; Matsuoka & Stolf, 2012; Thamoonlest et al., 2025). Consequently, plant population declines, productive land is underutilized, yields decrease, and economic losses accumulate over successive harvests (Amorim et al., 2022; Maldaner et al., 2025; Silva, 2025), making gap management important for promoting more sustainable production systems.

Methodological advances over the last decade have expanded the ability to detect and monitor sugarcane row gaps, including manual methods (Cavalcanti et al., 2023), onboard sensors (Maldaner et al., 2021), and approaches based on Unmanned Aerial Vehicle (UAV) (Melo et al., 2025; Thamoonlest et al., 2025). In addition, recent studies have shown that the spatiotemporal variability of sugarcane yield expresses distinct patterns of plant population reduction associated with row gaps, reinforcing the existence of clear cause-and-effect relationships at the row level within fields (Maldaner et al., 2024). Nevertheless, an important bottleneck remains: are row gaps concentrated in specific rows across different production contexts in a way that enables their optimized management? Although management decisions in sugarcane mills are still largely based on field-average indicators (e.g., field gap percentage), this approach does not reveal whether the productive and economic losses associated with row gaps are concentrated in a subset of rows or distributed uniformly throughout the field.

In this context, identifying critical rows, defined as those with the highest concentrations of linear gap lengths (LLG), may provide an objective basis for localized interventions and more efficient resource allocation. This study tested the hypothesis that specific sugarcane rows within a field concentrate most of the linear gap lengths and their associated economic and productive losses, consistent with the Pareto Principle (Gould, 1992). The objective was to identify rows that are critical in terms of LLG occurrence, making them priorities for site-specific interventions.

2. Material and Methods

2.1 Research location and data collection

The study was conducted in sugarcane fields located in the Center-South region of Brazil across a range of management conditions, varieties, soil classes, and harvest cycles. Initially, four case studies (CS) were evaluated, including one temporal analysis spanning two consecutive harvests, as summarized in Table 1. The datasets compiled for these case studies comprised yield data obtained from sugarcane harvesters, as well as the reconstruction of sugarcane rows and the spatial distribution of within-row gaps, both derived from row geometry extracted from UAV imagery.

Table 1. Geographic locations, agronomic practices, and yield metrics of the case studies.

Variables	Case study				
	1	2	3	4	
				Year 1	Year 2
Local	Nova Granada/SP,Brazil	Colina/SP,Brazil	Cajobi/SP,Brazil	Barretos/SP,Brazil	
Coordinates	20°32'02"S, 49°18'51"W	20°43'05"S, 48°32'38"W	20°52'47"S, 48°48'34"W	20°33'26"S, 48°34'04"W	
Variety	RB867515	RB985476	RB975201	CTC9003	
Harvest year/cutting nº	2021/3rd	2023/3rd	2023/1st	2023/3rd	2024/4th
N° Fields	2	3	3	1	
Area (ha)	214.08	40	26	21	
Density of yield points (points ha^{-1})	90385	1046	2254	745	859
Mean yield (Mg ha^{-1})	61.9	101.84	142.02	88.64	93.16
Soil class [a]	Oxisols	Ultisols	Ultisols	Oxisols	

[a] USDA Soil Taxonomy (Soil Survey Staff, 2022).

Yield data were obtained from single-row sugarcane harvesters using a commercial system that uses variations in harvester chopper feed pressure to spatially redistribute sugarcane production within the field, as described in detail by Maldaner et al. (2022), with an average acquisition frequency of 2 Hz. Subsequently, these data were filtered using the automatic filtering procedure developed by Silva et al. (2025).

Sugarcane rows and within-row gaps were derived from UAV-acquired imagery. Image acquisition was performed using an eBee UAV equipped with a SenseFly S.O.D.A. RGB camera (Sensor Optimised for Drone Applications), with a focal length of 25.40 mm and a spatial resolution of 20 megapixels, resulting in imagery with a ground sampling distance of 30 mm $pixel^{-1}$. Flight campaigns were planned using eMotion 3 software (AgEagle Aerial Systems Inc., Wichita, KS, USA) and conducted at an altitude of 100 m, with a front overlap of 70% and a side overlap of 60%. Image georeferencing was based on ground control points (GCPs), whose coordinates were collected using a Topcon GR-3 receiver operating with real-time kinematic (RTK) correction, providing positional accuracy of ±0.03 m. The mosaic image generation was carried out using PhotoScan v. 1.5 software (Agisoft LLC, St. Petersburg, Russia). The flight was conducted based on the height of the plants, when they reached between 0.60 and 1.20 m in growth at the beginning of the crop season, the visibility of the inter-row spacing, and the tillering phase of the ratoon cane.

Sugarcane rows and gaps were subsequently extracted from the RGB orthomosaic using InfoRow 2.0 software (SOMO, Piracicaba, Brazil). The workflow comprised six main steps, as described in Silva (2025). Gaps were identified based on plant spacing values greater than or equal to 0.6 m, following the threshold adopted by the sugarcane mill. For each field, the following metrics were obtained after processing: number of gaps, number of planting rows, linear length of rows (LLR), linear length of gaps (LLG), and percentage of gaps (*g* (%) – Stolf, 1986) (Table 2).

Table 2. Metric variables related to row reconstruction and gap identification, including the respective gap percentages for the case studies.

Case study	Variety	Harvest (cut)	nº gaps	$\sum LLG_{field}$ (m)	nº rows	∑LLR (m)	*g* (%)
1 – Field 1	RB867515	3rd	9983	12705.456	451	148860.54	8.5
1 – Field 2	RB867515	3rd	2817	3703.331	199	46044.40	8.0
2 – Field 1	RB985476	3rd	5617	6484.54	239	75487.98	8.6
2 – Field 2	RB985476	3rd	13536	18908.92	323	126700.13	14.9
2 – Field 3	RB985476	3rd	6359	8367.24	394	63590.90	13.2
3 – Field 1	RB975201	1st	4168	6299.47	338	75508.06	8.3
3 – Field 2	RB975201	1st	2812	3948.90	155	52425.68	7.5
3 – Field 3	RB975201	1st	3363	4679.76	133	44524.89	10.5
4 – Year 1	CTC9003	3rd	9486	13752.33	239	138647.817	9.9
4 – Year 2	CTC9003	4th	10181	27672.33	239	138647.817	20.0

$\sum LLG_{field}$: total linear gap length in the field; ∑LLR: total linear row length in the field; *g* (%): percentage of gaps.

2.2 Production not obtained due to gaps

To estimate the production not obtained due to gaps (P_g), three data layers were used: yield, gaps, and rows. A 0.60 m-spaced point grid was then created beneath the reconstituted sugarcane rows in QGIS v. 3.34.7 software (QGIS, 2024). Yield values from the yield layer were assigned to each grid point using the nearest neighbour approach, ensuring that every grid point was linked to a corresponding yield observation, as described by Silva (2025). A buffer was subsequently generated around each gap in the direction of the planting rows to include the yield points located within the gap area. P_g was then estimated according to Eq. (1).

$$P_g = Yg_i \times \frac{LLG_i}{\sum LLR} \tag{1}$$

where P_g is the not obtained production of a gap i (Mg); Yg_i is the estimated average yield within the gap i (Mg ha^{-1}), obtained by its nearest neighbors; LLG_i is the linear length of the gap i; and $\sum LLR$ is the total linear length of the rows of the given field (m ha^{-1}).

2.3 Costs of gaps

The financial costs of gaps were obtained as described by Silva (2025). The economic cost of the gap (GEC), comprising crop management and land leasing costs (Eq. 2), represented the costs incurred in the field due to gap occurrence. The opportunity cost of the gap (GOC, Eq. 3) was estimated as the economic value not obtained because of the absence of sugarcane production at the gap location. Opportunity cost refers to the value that is no longer gained when resources are allocated to a given use at the expense of other available alternatives (Hirschfeld, 1998).

$$GEC = LLG_i \times \left(C_{rental} + C_{cultural\ practices}\right) \tag{2}$$

where GEC is the gap economic cost (US$), LLG_i is the linear length of the gap (m) in the sugarcane field at a given location *i*, C_{rental} is the leasing cost (US$ linear meter^{-1}), $C_{cultural\ practices}$ is the cost of cultural practices (US$ linear meter^{-1}). Gap cost values were then transformed into gap cost per hectare by dividing $\sum GEC$ by the area of each field.

$$GOC = P_g \times Mg\ market\ price \tag{3}$$

where GOC is the gap opportunity cost (US$), P_g is the not obtained production of a gap in each location i (Mg) (obtained by Eq. 1), $Mg\ market\ price$ is the average selling price of 1 Mg of sugarcane (US$ Mg^{-1}).

The economic analysis was based on data from the Brazilian sugarcane sector and converted to US$ using official government exchange rates at the time of the study (1 US$ = 5.16, 4.99 and 5.39 BRL in 2021, 2023 and 2024, respectively; Table 2). Costs of operation, such as operation costs, were not considered in this study; this partial budget approach ensures a targeted evaluation of the key economic drivers.

Table 3. Cost data used for the economic analysis of sugarcane row gaps.

		2021		2023		2024	
Cost	Variables	US$ ha^{-1}	US$ linear $meter^{-1}$ [c]	US$ ha^{-1}	US$ linear $meter^{-1}$	US$ ha^{-1}	US$ linear $meter^{-1}$
GEC	Cultural practices[a]	721.11	0.11	591.39	0.089	510.07	0.077
	Leasing[a]	449.20	0.070	475.88	0.071	436.78	0.066
GOC	1 Mg market price[b]	24.95		26.05	–	23.85	–

a: Data obtained from the Associação Rural dos Fornecedores e Plantadores de Cana do Vale do Paranapanema (in Portuguese) (ASSOCANA, 2023; 2024), b: data obtained from the Conselho dos Produtores de Cana de Açúcar, Açúcar e Etanol do Estado de São Paulo (in Portuguese) (CONSECANA, 2023; 2024), c: constant values, considering uniform management.

2.4 Determining the critical rows of sugarcane

For each field, the LLG values of each row were summed, obtaining the total gap length per sugarcane row ($\sum LLG_{row}$, in m). Next, the rows were sorted in descending order according to their total LLG values, from the row with the highest $\sum LLG_{row}$ to rows with no gaps ($\sum LLG_{row} = 0$). Based on the Pareto Principle (Gould, 1992), which states that a minority of causes generates the majority of effects, the identification of critical rows considered the cumulative distribution of LLG among the rows of the field. For this purpose, each row *R*'s percentage contribution relative to the field's total LLG was calculated (Eq. 4).

$$pct_R = \frac{(\sum \mathrm{LLG}_{row})_R}{\sum_{j=1}^{N} (\sum \mathrm{LLG}_{row})_j} \times 100 \quad (4)$$

The corresponding cumulative percentage was obtained according to Eq. 5.

$$cumulative\ pct_R = \sum_{k=1}^{R} pct_k \quad (5)$$

where pct_R is the percentage relative to the field's total gap length (%), *N* is the total number of rows, *j* is the summation index of the rows.

The classification of critical rows was then performed based on the behavior of the cumulative percentage along the ranking, highlighting the rows responsible for the greatest concentration of LLG in the field, while the others were considered non-critical. Subsequently, for each row, the sums of P_g, GEC, and GOC were also obtained, and their cumulative distributions were analyzed based on the classification previously established for LLG.

2.5 Extra datasets

Additionally, 10 extra datasets from different farms and management contexts were evaluated using the same approaches described previously (Table 4). However, in order to validate the approach and the Pareto-type relationship, only the row reconstruction and gap layers were used, without the yield data layer and the variables related to this layer (P_g and GOC), in order to simplify the process.

Table 4. Geographic locations, agronomic practices, of the dataset extras.

Dataset	Coordinates	Area (ha)	Variety	Harvest (cut)	$\sum LLG_{field}$ (m)	nº of rows	∑LLR (m)	% *g*
1	20°37'00"S, 49°27'50"W	32.17	RB966928	6th	24290.71	397	211866.05	12
2	20°10'33"S, 48°41'20"W	22.84	RB975242	5th	77558.28	351	150057.48	52

3	20°29'55"S, 48°56'41"W	48.32	RB966928	6th	62012.56	579	319684.74	19
4	20°44'14"S, 48°54'53"W	24.46	RB975201	4th	11869.66	308	162276.56	7
5	20°44'14"S, 48°54'53"W	14.36	RB966928	6th	12404.05	235	94164.19	13
6	20°44'14"S, 48°54'53"W	23.92	RB966928	2nd	16902.15	318	159192.90	11
7	20°44'14"S, 48°54'53"W	19.32	CTC9003	3rd	11111.85	310	128063.45	9
8	20°52'47"S, 48°48'34"W	13.89	RB975201	8th	18498.96	309	90951.06	20
9	20°10'33"S, 48°41'20"W	17.58	RB975952	4th	7021.11	211	116050.95	6
10	20°29'55"S, 48°56'41"W	24.66	CV7870	3rd	29030.43	442	163164.30	18

$\sum LLG_{field}$: total linear gap length in the field; $\sum LLR$: total linear row length in the field; *g* (%): percentage of gaps, calculated following Stolf (1986).

2.6 Statistical analyses

Descriptive statistics were performed for the obtained variables, including the minimum, maximum, mean, median, and skewness values. In this study, the inequality in the distribution of LLG among sugarcane rows was described by the Gini coefficient (G), a widely used measure to quantify dispersion in a population (Baydil et al., 2025). To construct the Lorenz curves and calculate the associated Gini coefficient, the rows within each field were ranked from the lowest to the highest sum of LLG, and the cumulative fraction of the field's total LLG was plotted as a function of the cumulative fraction of the number of rows. The line y = x represents the case of perfect equality. G quantifies the area between the Lorenz curve and this line of perfect equality, expressed as a fraction of the total area under the line y = x (Zhao et al., 2025), as shown in Eq. 6.

$$G = \frac{\sum_{i=1}^{n}(2i-n-1)x_i}{n\sum_{i=1}^{n}x_i} \quad (6)$$

where G is the Gini coefficient, x_i is the value of $\sum LLG_{row}$ for *i*-th row, after sorting in ascending order, *n* is the total number of rows. The Gini coefficient ranges from [0, 1], being equal to 0 when all rows have the same LLG value and tending to 1 when LLG is more concentrated in a reduced set of rows.

3. Results and Discussion

The distribution of LLG among rows was uneven in most of the sugarcane fields evaluated, as shown in Table 5. In the case studies, with the exception of the second year of the temporal assessment, 70% of the field LLG was accumulated in 30% to 40% of the rows, associated with G between 0.39 and 0.54, indicating greater inequality in the distribution of LLG among rows. In field 2 of case study 1, for example, 59 of the 199 rows concentrated 70% of the field's LLG, with G = 0.54. This result shows that the highest LLG concentrations occurred in a restricted subset of rows, in line with the Pareto Principle (Gould, 1992), which states that most effects tend to be associated with a relatively small proportion of causes, although the magnitude of this relationship may vary.

Table 5. Summary of row-gap concentration, Gini coefficient, and skewness across case studies and extra datasets.

Group	ID	Total rows (n)	Critical rows, n (%)	$\sum LLG_{row}$ in critical rows (m) (% of field total)	G	Skewness
Case study 1	Field 1	451	180 (40% of rows)	8896.61 (70% of $\sum LLG_{field}$)	0.43	1.30
Case study 1	Field 2	199	59 (30% of rows)	2605.84 (70% of $\sum LLG_{field}$)	0.54	2.15
Case study 2	Field 1	239	96 (40% of rows)	4555.74 (70% of $\sum LLG_{field}$)	0.42	1.92
Case study 2	Field 2	323	104 (32% of rows)	13254.87 (70% of $\sum LLG_{field}$)	0.51	1.89
Case study 2	Field 3	394	134 (34% of rows)	5876.37 (70% of $\sum LLG_{field}$)	0.49	1.66
Case study 3	Field 1	338	110 (33% of rows)	4466.64 (70% of $\sum LLG_{field}$)	0.51	2.38
Case study 3	Field 2	155	55 (35% of rows)	2772.73 (70% of $\sum LLG_{field}$)	0.49	2.31
Case study 3	Field 3	133	53 (40% of rows)	3304.27 (70% of $\sum LLG_{field}$)	0.43	1.60
Case study 4	Year 1	239	96 (40% of rows)	9680.97 (70% of $\sum LLG_{field}$)	0.39	1.23
Case study 4	Year 2	239	125 (52% of rows)	19469.09 (70% of $\sum LLG_{field}$)	0.25	0.89

Extra dataset	1	397	161 (41% of rows)	17035.03 (70% of $\sum LLG_{field}$)	0.41	0.77
Extra dataset	2	351	202 (58% of rows)	54623.69 (70% of $\sum LLG_{field}$)	0.18	-0.14
Extra dataset	3	579	263 (45% of rows)	43413.67 (70% of $\sum LLG_{field}$)	0.35	1.17
Extra dataset	4	308	139 (45% of rows)	8403.43 (70% of $\sum LLG_{field}$)	0.36	2.38
Extra dataset	5	235	106 (45% of rows)	8775.22 (70% of $\sum LLG_{field}$)	0.35	0.95
Extra dataset	6	318	123 (39% of rows)	11868.29 (70% of $\sum LLG_{field}$)	0.42	0.89
Extra dataset	7	310	101 (33% of rows)	7808.19 (70% of $\sum LLG_{field}$)	0.49	1.38
Extra dataset	8	316	128 (42% of rows)	12973.21 (70% of $\sum LLG_{field}$)	0.39	1.13
Extra dataset	9	211	92 (44% of rows)	4962.46 (70% of $\sum LLG_{field}$)	0.37	1.85
Extra dataset	10	442	149 (34% of rows)	20316.01 (70% of $\sum LLG_{field}$)	0.50	1.39

$\sum LLG_{row}$: total linear gap length in the row; $\sum LLG_{field}$: total linear gap length in the field; G: Gini coefficient. Gray-shaded lines indicate ratoon cane ≥ 4th cut.

Even under different management practices, sugarcane varieties, soil classes, harvest cycles, and traffic directions across the rows, the analysis showed that, in the case studies, a minority of rows was responsible for most of the field LLG, the associated financial costs, and the sugarcane production not obtained due to these gaps (Fig. 1). In field 1 of case study 3, for example, 33% of the rows were responsible for at least 70% of the LLG, and these same rows also represented approximately 70% of P_g, GEC, and GOC.

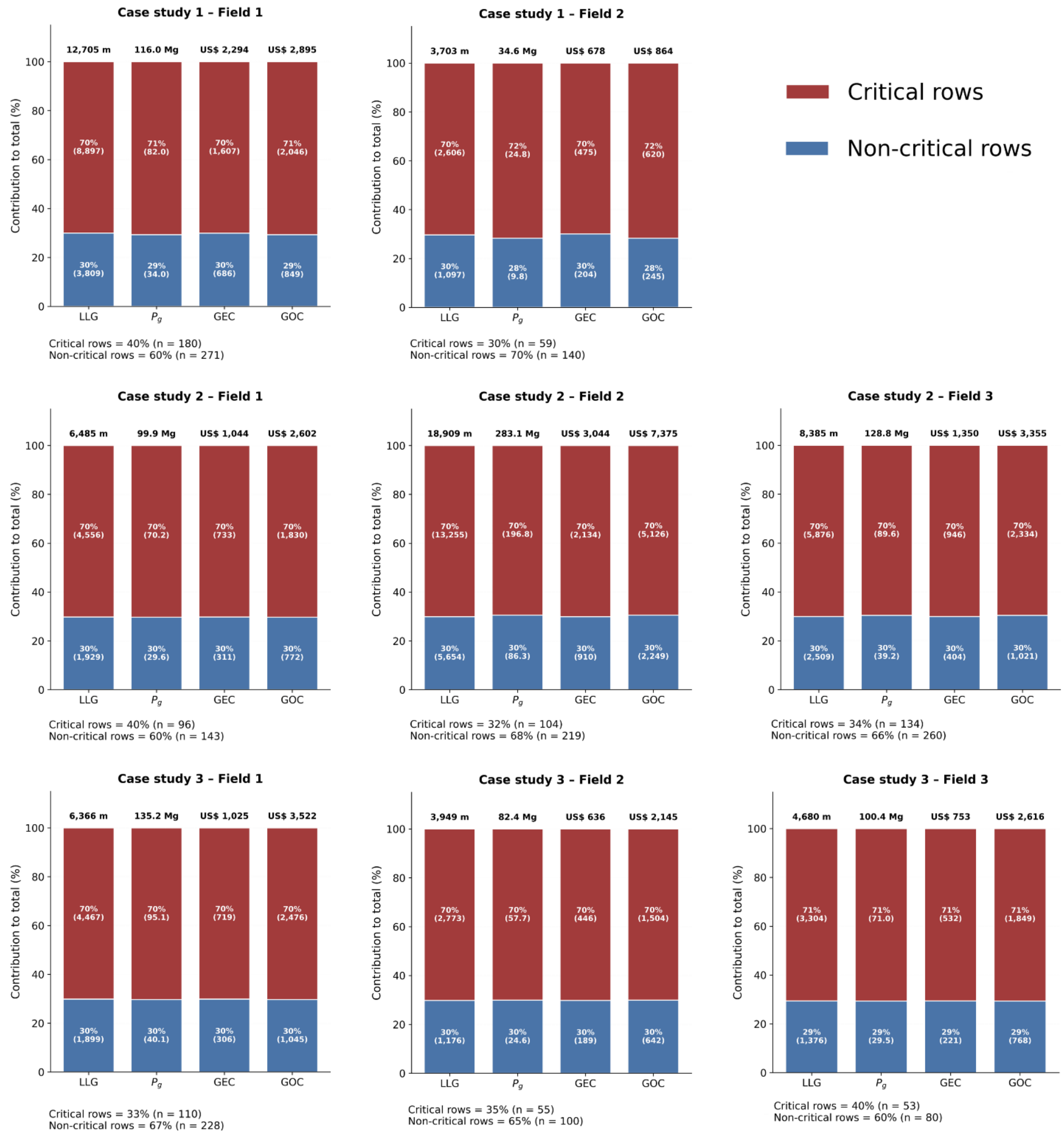

Fig 1. Contribution of critical and non-critical sugarcane rows to linear gap length (LLG), production not obtained due to gaps (Pg), gap economic cost (GEC), and gap opportunity cost (GOC) across the investigated case studies. Stacked bars show the relative contribution (%) and absolute values of critical and non-critical rows to total LLG, Pg, GEC, and GOC. The proportion and number of rows belonging to each group are indicated below each panel.

In the temporal assessment (CS 4), in year 1 (3rd cut), 96 of the 239 rows, corresponding to 40% of the total, concentrated 70% of the LLG, with G equal to 0.39; in the following harvest (year 2, 4th cut), 125 rows, or 52%, were required to reach the same cumulative fraction of LLG, with G reduced to 0.25. This result indicates a lower concentration of LLG in specific rows in the more advanced crop cycle and suggests a degradation of the Pareto-like pattern as the sugarcane field advances in number of cuts. The mapping of the temporal scenario is shown in Fig. 2, where this spatial hierarchy can be seen: the dark red lines indicate the most critical rows, corresponding to those with the highest summed LLG values. The color gradient shifts to light red in the less critical rows and to blue in the non-critical rows.

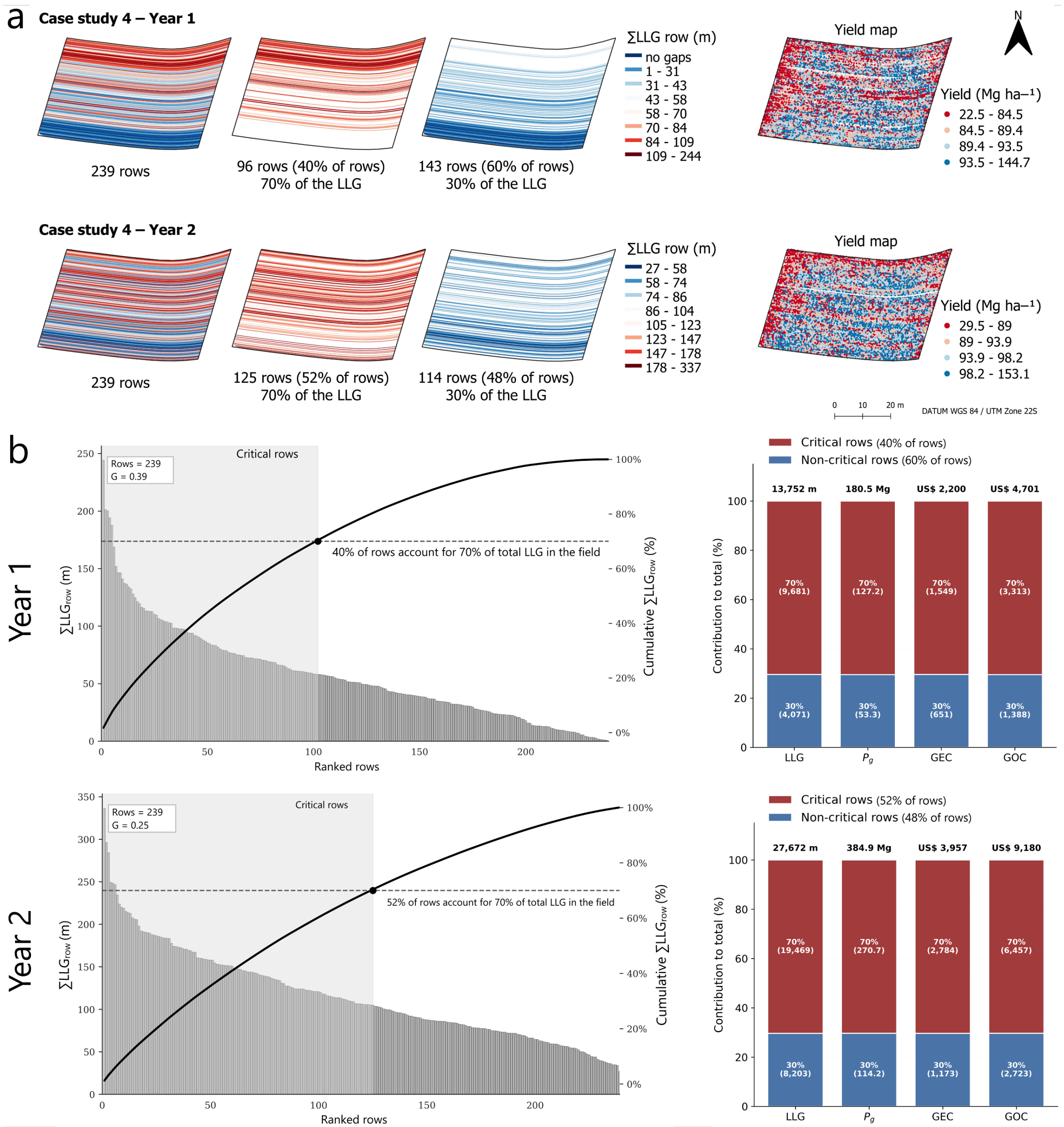

Fig 2. Spatial distribution of sugarcane row gaps and associated impacts in case study 4 during two consecutive harvest years. (a) Maps of linear gap length (LLG) per row and yield maps for year 1 and 2. Rows were ranked according to the cumulative LLG and classified into critical rows (responsible for 70% of total LLG) and non-critical rows (remaining 30% of total LLG). (b) Pareto curves showing the cumulative distribution of LLG among ranked rows, highlighting the proportion of rows required to account for 70% of total LLG in each year. Bar charts show the contribution of critical and non-critical rows to total LLG, production not obtained due to gaps (P_g), gap economic cost (GEC), and gap opportunity cost (GOC). $\sum LLG_{row}$: total linear gap length in the row; G: Gini coefficient.

Fig. 2 showed that the most critical rows were normally located in low-yield zones. Thus, two layers obtained through different field methods (yield — via sugarcane harvester; gaps — UAV) revealed a spatial pattern of gap occurrence associated with reduced yield. Factors that may contribute to this phenomenon include parallelism and travel angle, which increase machinery traffic over the plants and favor damage to shoots, terrain slope, the presence of weeds, suboptimal nutrient availability, the occurrence of pests and diseases (Mahadea-Nemdharry et al., 2025; Maldaner et al., 2025), as well as row length, since longer rows have a higher probability of continuous gaps.

The pattern of LLG concentration relative to the number of rows is also evidenced by the Lorenz curves of the case studies and extra datasets (Fig. 3). In the case studies, the scenarios with higher G values remained farther from the line of perfect equality, whereas CS 4 – Year 2 showed a curve closer to this reference, consistent with its lower G value and with the need for a larger fraction of rows to make up the same cumulative proportion of LLG. For the extra datasets, the same LLG concentration pattern was achieved with 33% to 58% of the rows, while G values ranged from 0.18 to 0.50. Datasets 7 and 10, both from 3rd cut, maintained a high concentration of LLG in a limited number of rows, with 33% and 34% of the rows accounting for 70% of the LLG and G values of 0.49 and 0.50, respectively.

In contrast, in fields at more advanced production stages, dataset 2 (5th cut) required 58% of the rows to reach the same cumulative fraction, with G equal to 0.18. This result shows that, in more advanced ratoon cycles, the curves tended to move closer to the line of equality, suggesting a more homogeneous distribution of LLG along the rows within the field. These results are also consistent with the skewness values of the LLG distribution, which were lower in sugarcane fields in more advanced crop cycles (highlighted in gray in Table 5), compared with the relatively higher and more pronounced values observed in the initial crop cycles, indicating a predominance of right-skewed distributions.

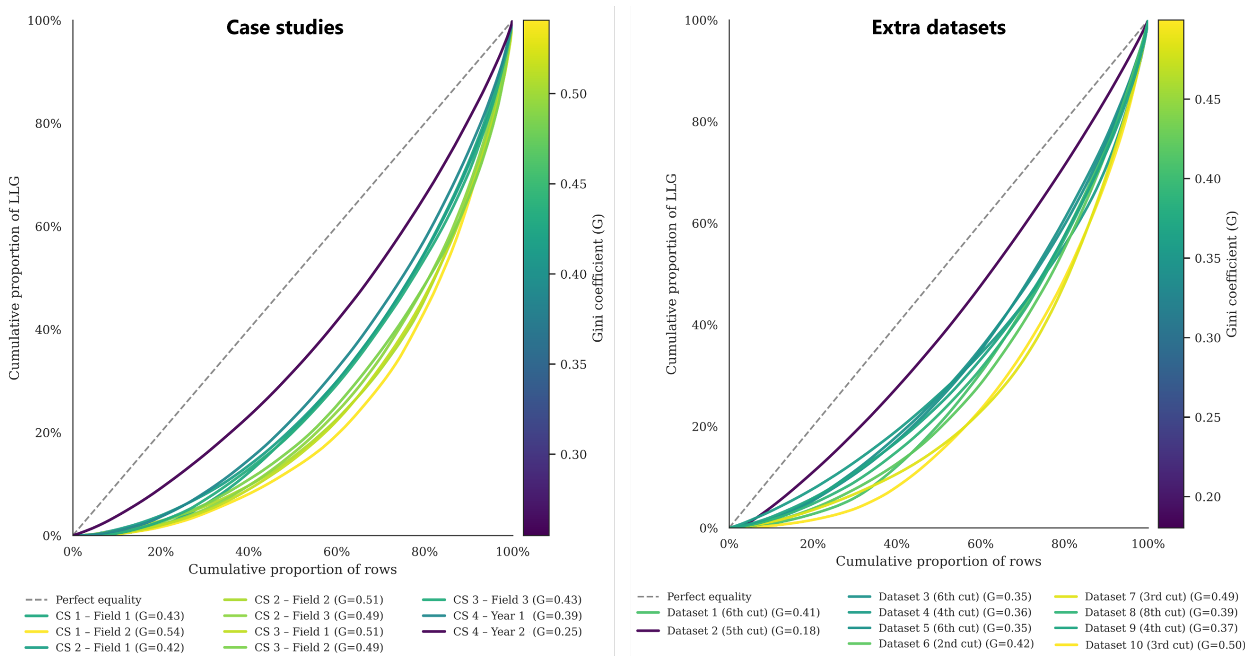

Fig 3. Curves of Lorenz for the case studies (left) and extra datasets (right). The x-axis represents the cumulative proportion of rows, and the y-axis represents the cumulative proportion of LLG. The Lorenz curve reflects the degree of dispersion in the distribution of LLG across sugarcane rows. When the curve coincides with the line of perfect equality, all rows have the same LLG value, indicating a completely uniform distribution of gap lengths.

The proposed approach in this study contributes to a decision-support system aimed at targeted row-level interventions, such as localized replanting operations and ON/OFF input application systems. The feasibility of replanting should be evaluated on a case-by-case basis by the manager and the sugarcane mill, considering the stage of the crop and the nature of the observed gaps. In sugarcane fields in the first cycles, localized replanting may be a more suitable alternative; however, the economic feasibility and financial return of this operation over the harvest seasons need to be assessed. Whereas in areas with more advanced crop cycles, it may be more appropriate to propose renovation actions, using the mapping of critical rows to guide this operation and define the highest-priority fields.

In addition, the identification of critical rows opens up opportunities to investigate the causes of the gaps and better understand the origin of these occurrences. In some cases, the gaps may be related to site-specific conditions that require targeted local management, such as the presence of weeds, pests, and soil compaction. In other cases, the gaps may be associated with low-yield areas due to intrinsic soil and terrain characteristics, such as texture and relief/slope, and, in these scenarios, it may be more advantageous to adopt "coexistence actions" in the most affected rows.

From an operational perspective, identifying the rows with the highest concentration of gaps can facilitate targeted planning, optimizing agricultural operations and logistics, such as route planning. Since operators need to travel along entire rows due to limited maneuverability within the field, concentrating interventions on the critical rows can reduce maneuvering requirements, fuel consumption, and plant damage caused by machine traffic. In the long run, implementing these actions can contribute to the sustainability and responsibility of sugarcane cultivation, aligning with global goals such as SDG 2 (Zero Hunger), SDG 12 (Responsible Consumption and Production), and SDG 13 (Climate Action) (UN, 2015). From an economic perspective, the manager's decision can prioritize intervention areas with greater potential return on investment (Farinelli et al., 2018), in order to minimize gaps at the lowest possible cost.

Conclusions

This study confirmed the hypothesis that specific rows within the field concentrate most of the linear gap lengths and the associated productive and economic losses, in accordance with the Pareto Principle. The Lorenz curves and Gini coefficients showed that this concentration is more pronounced in the initial crop cycles (up to the third harvest), in which the critical rows are more clearly defined, and tends to become more diffuse in more advanced ratoon cycles (from the fourth harvest onward), with a weakening of the Pareto-like pattern. The results demonstrate the potential of the proposed approach to identify critical rows and support targeted interventions at the row level. From a management perspective, the approach supports the prioritization of localized replanting in sugarcane fields in the first harvest cycles and renovation planning in fields with more advanced cycles. This contributes to improved production efficiency and better resource allocation.

Acknowledgments

This work was supported by the Coordenação de Aperfeiçoamento de Pessoal de Nível Superior (CAPES, Finance Code 001), and also financial support promoted by the Conselho Nacional de Desenvolvimento Científico e Tecnológico (CNPq, grant number 306177/2021-8). The authors would like to acknowledge Solinftec and the Tereos Group for their invaluable support in data acquisition.

References

Amorim, F. R., Patino, M. T. O., & Santos, D. F. L. (2022). Soil tillage and sugarcane planting: an assessment of cost and economic viability. Scientia Agricola, 79(1). https://doi.org/10.1590/1678-992X-2019-0317

Associação Rural dos Fornecedores e Plantadores de Cana do Vale do Paranapanema (ASSOCANA) (2023; 2024). Custos. https://www.assocana.com.br/ custos.php (accessed on December 2025).

Baydil, B., la Peña, V. H., Zou, H., & Yao, H. (2025). Unbiased estimation of the Gini coefficient. Statistics & Probability Letters, 222,110376. https://doi.org/10.1016/j.spl.2025.110376.

Cavalcanti, R. Q., Rolim, M. M., Lima, R. P., Ortiz, P. F. S., Pedrosa, E. M. R., & Rodrigues, J. A. M. (2023). Sugarcane Row Gaps Assessment over Successive Burned and Unburned Annual Harvests. Agronomy, 13(10), 2545. https://doi.org/10.3390/agronomy13102545

Companhia Nacional de Abastecimento (CONAB) (2026). Acompanhamento da Safra Brasileira: Cana-de-açúcar. https://www.gov.br/conab/pt-br/atuacao/informacoes-agropecuarias/safras/safra-de-cana-de-acucar/arquivos-boletins/1o-levantamento-safra-2026-

27/1o-levantamento-safra-2026-27 (accessed on April 2026).

Conselho dos Produtores de Cana de Açúcar, Açúcar e Etanol do Estado de São Paulo (CONSECANA) (2023; 2024). Custo operacional da lavoura de cana-de-açúcar. https://www.udop.com.br/u_cana/tabela_consecana_saopaulo.pdf (accessed on December 2025).

Farhate, C. V. V., Souza, Z. M., Oliveira, S. R. M., Tavares, R. L. M., & Carvalho, J. L. N. (2018). Use of data mining techniques to classify soil CO2 emission induced by crop management in sugarcane field. PLOS ONE, 13(3), e0193537. https://doi.org/10.1371/journal.pone.0193537

Food and Agriculture Organization Statistics (FAOSTAT) (2026). Crops and livestock products. https://www.fao.org/faostat/en/#data/QCL (accessed on April 2026).

Gould, W. A. (1992). Problem Solving – Pareto Principle. In W. A. Gould (Eds.), Total Quality Management for the Food Industries (pp. 43-47). Sawston: Woodhead Publishing. https://doi.org/10.1016/B978-1-84569-601-6.50015-3.

Guhan, V., Annadurai, K., Easwaran, S., Marimuthu, M., Balu, D., Vigneswaran, S., & Navinkumar, C. (2024). Assessing the impact of climate change on water requirement and yield of sugarcane over different agro-climatic zones of Tamil Nadu. Scientific Reports, 14, 8239. https://doi.org/10.1038/s41598-024-58771-8

Hirschfeld, H. (1998). Engenharia Econômica e Análise de Custos. (6th ed). São Paulo: Atlas.

Mahadea-Nemdharry, R., Doorga, J. R. S., Busawon, K., & Seeruttun, S. (2025). Enhancing sugarcane field management in a tropical island: A comparative analysis of mapping gaps in sugarcane fields using drone and satellite imageries. Remote Sensing Applications: Society and Environment, 38, 101570. https://doi.org/10.1016/j.rsase.2025.101570

Maldaner, L. F., J. P. Molin, C. T. S. Dias, & E. R. O. Silva. (2025). When ratoon longevity matters: Spatial and temporal analysis of sugarcane plant population patterns using features extracted from UAV images. Remote Sensing Applications: Society and Environment, 39, 101703. https://doi.org/10.1016/j.rsase.2025.101703

Maldaner, L. F., Canata, T. F., & Molin, J. P. (2022). An Approach to Sugarcane Yield Estimation Using Sensors in the Harvester and ZigBee Technology. Sugar Tech, 24, 813–821. https://doi.org/10.1007/s12355-021-01050-x

Maldaner, L. F., Molin, J. P., Martello, M., Tavares, T. R., & Dias, F. L. F. (2021). Identification and measurement of gaps within sugarcane rows for site-specific management: Comparing different sensor-based approaches. Biosystems Engineering, 209, 64–73. https://doi.org/10.1016/J.BIOSYSTEMSENG

Matsuoka, S., & Stolf, R. (2012). Sugarcane tillering and ratooning: key factors for a profitable cropping. In J.F. Gonçalves and K.D. Correia. (Eds.), Sugarcane: Production, Cultivation and Uses (pp. 137-157), New York: Nova Science Publishers.

QGIS.org. (2024). QGIS Geographic Information System. QGIS Association. https://www.qgis.org (accessed on February 2026)

Raza, M. A., Din, A. M. U., Gul, H., Zhiqi, W., Yasin, H. S., Khalid, M. H. B., Iqbal, N., Saeed, A., Bukhari, B., Dosary, M. A. A., Juan, C., Liang, X., Luo, S., van der Werf, W., Feng, Y., Qin, R., & Zhongming, M. (2024). Sugarcane/soybean intercropping enhances crop productivity, nutrient uptake, and net economic return with reduced inputs. Field Crops Research, 314, 109428. https://doi.org/10.1016/j.fcr.2024.109428

Silva, E. R. O. (2025). Operational and economic impacts of sugarcane row gaps. (Doctoral Thesis). Universidade de São Paulo, Escola Superior de Agricultura Luiz de Queiroz, Piracicaba.

Silva, E. R. O., Molin, J. P., Wei, M. C. F., & Canal Filho, R. (2024). Automatic Filtering of Sugarcane Yield Data. AgriEngineering, 6(4), 4812–4830.

https://doi.org/10.3390/agriengineering6040275.

Soil Survey Staff. (2022). Keys to soil taxonomy (13th ed.). USDA Natural Resources Conservation Service. https://www.nrcs.usda.gov/sites/default/files/2022-09/Keys-to-Soil-Taxonomy.pdf

Stolf, R. (1986). Metodologia de avaliação de falhas nas linhas de cana-de-açúcar. STAB, 4, 22–36.

Thamoonlest, W., Posom, J., Saikaew, K., Phuphaphud, A., Chinapas, A., Panduangnat, L., & Saengprachatanarug, K. (2025). Forecasting gaps in sugarcane fields containing weeds using low-resolution UAV imagery based on a machine-learning approach. Smart Agricultural Technology, 10, 100780. https://doi.org/10.1016/j.atech.2025.100780

United Nations (UN) (2015). The 17 goals. https://sdgs.un.org/goals (accessed on January 2026).

Zhao, M., Xiao, P., Liang, C., Wang, C., Li, B., & Zheng, W. (2025). A new index based on Gini coefficient for evaluating the distribution uniformity of environmental parameters in buildings. Building and Environment, 278, 112910. https://doi.org/10.1016/j.buildenv.2025.112910.